Catalysis Letters Vol. 104, Nos. 3–4, November 2005 (© 2005)
DOI: 10.1007/s10562-005-7939-7

Copper-based catalysts for synthesis of methylamines: the effect of the metal and the role of the support

Nielson F.P. Ribeiro[a], Cristiane A. Henriques[b], and Martin Schmal[a,*]

[a]*NUCAT/PEQ/COPPE, Universidade Federal do Rio de Janeiro, C.P. 68502, 21945-970, Rio de Janeiro, Brazil*
[b]*DQA/Instituto de Química, Universidade do Estado do Rio de Janeiro, Rua São Francisco Xavier, 524, CEP, 20559-900, Rio de Janeiro, Brazil*

Received 15 February 2005; accepted 2 July 2005

Three Cu-based catalysts supported in different materials were prepared. The textural properties showed that the thermal treatment and the presence of CuO resulted in decrease of BET area. The surface areas of the Cu on alumina and zeolite decay with Cu addition, which can be attributed to the formation of CuO particles, blocking the pores. Contrary, the based like-hydrotalcite catalysts surface areas increased, which may be attributed to the destruction of the structure and formation of oxide mixtures. The acid sites with moderate strength favored the methylamines production, due to the easier desorption of products. The metallic sites affect the reaction since they provide a decrease in desorption temperature of the amines and enhance the disproportionation. The metallic sites in the based like-hydrotalcite catalysts Cu/Mg–Al enhance the formation of methylamines. The Cu/Al_2O_3 was more active and stable than the other Cu based catalysts.

KEY WORDS: methylamines; amination of methanol; copper catalysts; zeolite; like-hydrotalcite; alumina; TPSR.

1. Introduction

Amines are organic compounds derived from ammonia after successive changes of hydrogen atoms by alkyl or aryl groups. The amines are very important in the market of chemical intermediates, and methylamines (MA) are the most important in these markets, used in different industrial applications, such as, paint industries, water treatment, insecticide and pesticide production, as well as, ionic change resin, mineralize agents, animal food, NO_x reduction, etc.

The commercial process of MA synthesis is the amination of alcohols in the gas phase through an exothermic reaction, using methanol and ammonia as reagents in the presence of acid catalysts [1]. The products of this reaction are monomethylamine (MMA), dimethylamine (DMA) and trimethylamine (TMA), and in thermodynamic equilibrium TMA is the main product (molar ratio 17/21/62 MMA:DMA:TMA; 673 K and N/C = 1) [2]. However, the most interesting commercial products are MMA and DMA [3]. This is clearly shown by the World demand (molar ratio 34/53/13 in the EUA, 26/59/15 in Western Europe and 14/78/8 in Japan).

In response to the real demand of the market and because the thermodynamic equilibrium, the industrial processes are usually carried out in two reactors for MA production. One reactor utilizes an oxide metallic mixture supported on alumina and the other a zeolite catalyst for the disproportionation of TMA molecules [4]. However, the separation and subsequent recycle of TMA is still a necessary step to increase MMA and DMA selectivities. This step is much harmful from economic viewpoint, due to the increasing costs of the process, because the separation of TMA is difficult and expensive, since MMA, DMA and TMA, together with ammonia is an azeotropic mixture [5].

In the current literature all catalysts did not reach the required molar ratio in the industry, although further efforts are being done in the way to optimize conditions of process and developing catalysts to maximize MMA and DMA production. The main focus was to adjust textural and physical–chemical properties of zeolite materials, making a balance between the shape-selective and acidity, which should increase the activity and selectivity and decrease deactivation. Other alternative catalysts were synthesized, such as carbon composites, according to Peréz-Mendoza *et al.* [3] or hydrotalcites modified with transition metals, synthesized by Auer *et al.* [6] and Carja *et al.* [7], that improved MMA and DMA selectivity.

The objective of this work is to verify the effect of the metal and the role of the support on the product distribution and to determine the morphology and physical–chemical properties of different supported copper catalysts, as well as to evaluate the nature of the metallic species present during the amination reaction with methanol.

2. Experimental

2.1. Catalysts preparation

Zeolite HZSM-5 (SAR = 23.3) was used for the preparation of Cu catalysts using ion exchange, as

* To whom correspondence should be addressed.
E-mail: schmal@peq.coppe.ufrj.br

1011-372X/05/1100–0111/0

described elsewhere [8]. First, the zeolite was calcined in flowing air (50 cm^3/min) at 803 K for 4 h at 5 K/min, and after washing with a solution of 10% sodium nitrate was exchanged with Cu ions using a solution of copper nitrate. Then, the pH was adjusted to 7.0 using a concentrated solution of ammonium hydroxide, evacuated, filtered immediately and dried at 383 K for 24 h. Finally, the sample was calcined in flowing air (50 cm^3/min) at 773 K for 6 h and at a heating rate of 1 K/min.

The base like-hydrotalcite was synthesized by co-precipitation method, as describe elsewhere [9]. The sample was prepared containing magnesium and aluminum in its structure, using the solutions $Mg(NO_3)_2{\cdot}6H_2O/Al(NO_3)_3{\cdot}9H_2O$ (molar ratio $Mg^{+2}/Al^{+3}=3$; $[Al^{+3}/(Mg^{+2}+Al^{+3})]=0.25$ and Al + Mg = 1.5 M) and $NaCO_3/NaOH$ (molar ratio $CO_3^{-2}/A1^{+3}=0.375$ and $Na^{+}/Al^{+3}=0.157$). Copper was added by wet impregnation with a solution of copper nitrate. This sample was dried at 383 K for 24 h and calcined in flowing air (50 cm^3/min) at 773 K for 6 h, at 1 K/min.

The last catalyst was synthesized by wet impregnation method using alumina supports. Firstly, alumina was calcined in flowing air (50 cm^3/min) at 833 K for 16 h. Then copper was added similarly.

2.2. Characterization

N_2 adsorption at 77 K. The textural properties were obtained in an ASAP 2000 apparatus (Micromeritics) under vacuum at 473 K. BET surface areas were determined by nitrogen isotherms at 77 K.

X-ray fluorescence (XRF). The chemical compositions of synthesized samples were determined by XRF spectroscopy (Rigaku – RIX 3100).

X-ray diffraction (XRD). X-ray powder diffraction patterns were recorded on a Rigaku – Miniflex diffractometer using monochromatic CuKα, (30 kV e 15 mA) over a 2θ range from 2 to 90 °.

Temperature-programmed reduction (TPR). Apparatus and methodology were described elsewhere [8]. The samples were dehydrated at 503 K under flowing Ar before the reduction. A mixture of 1.74% hydrogen in argon flows at 30 mL/min through the sample, raising the temperature at a heating rate of 10 K/min up to 1073 K.

Temperature-programmed desorption of ammonia (TPD-NH_3). The analysis was performed using a mass spectrometer QMS-200 (BALZER), The sample was reduced at 773 K before adsorption of ammonia at 473 K and then desorbed under flow of He (50 mL/min), increasing the temperature up to 803 K (rate 10 K/min). The ratio $m/e=15$ was used for quantification of ammonia.

Infrared of the reaction in situ (FTIR in situ). The analysis was carried out in a Perkin–Elmer apparatus model System 2000 FTIR with the samples analyzed on self-made pastille. The experiments started by adsorptions of methanol and ammonia at room temperature after reduction, as described above. The reactions *in situ* were performed at 623 K with closed cell. Before each step the sample was evacuated and the IR spectrum registered.

2.3. Catalyst testing

Temperature-programmed surface reaction (TPSR). The reaction was carried out in a fixed-bed flow-type Pyrex reactor loaded with 10 mg of active phase, under atmospheric pressure. The methanol was carried out using a saturator and flowing He at 303 K, and ammonia flows with a mixture 4% NH_3/He (v/v). The products were analyzed by on-line mass spectrometer QMS-200 (BALZER). The compounds were identified using calibrated mass elements ($m/e=30$, 44 and 58 for MMA, DMA and TMA, respectively). Here, we adopted two experimental procedures. First, the sample was reduced with H_2 (30 mL/min) at 10 K/min from RT up to 773 K and held constant during 45 min. Next, the sample was cooled down to 423 K under H_2 flow and then to room temperature under He flow at 50 cm^3/min. In the first procedure, ammonia was adsorbed flowing 4% NH_3/He (v/v) (50 cm^3/min). After stabilization, ammonia was removed with He at 50 cm^3/min. Methanol was introduced in the reactor with He flow through a saturator at 298 K, until stabilization ($m/e=30$). Then, the temperature rose at a heating rate of 10 K/min up to 803 K. The second procedure was similar, but methanol was first adsorbed followed by ammonia flow.

Reaction. The reaction was carried out in a fixed-bed flow-type reactor loaded with 50 mg of catalyst. The sample was reduced with H_2 (30 mL/min) at 10 K/min up to 773 K, keeping constant for 45 min, and cooled down to the reaction temperature. The reactants were introduced at 43 mL/min and atmospheric pressure. Methanol in a saturator at 303 K was introduced flowing N_2 and blended with ammonia fluxing a 20% NH_3/N_2 (v/v) mixture. The feed molar ratio nitrogen/carbon (N/C) was 1.0. Products were analyzed by gas chromatography using a Varian model 3300, equipped with flame ionization detector and a cp-Volamine capillary column.

3. Results and discussion

3.1. Composition and morphology

The chemical composition results are presented in table 1. The metal contents were close to the nominal values, with exception of the Cu/Mg–Al catalyst, which was little higher due to the loss of about 40% of water of this material (like-hydrotalcite) after calcination. According to Beutel *et al.* [10] the green color of this catalyst indicates the presence of oxygen copper

Table 1
Chemical composition of different catalysts

Catalysts	% Cu (p/p) real	% Cu (p/p) nominal	Color^{BC}	Color^{AC}
Cu/HZSM5	4.2	4	Light blue	Gray
Cu/Mg–Al	7.2	4	Light blue	Light green
Cu/Al_2O_3	4.2	4	Light blue	Light blue with dark gray points

Superscripts BC and AC refer to, before and after calcination, respectively.

complex $[Cu–O–Cu]^{2+}$. On the other hand, the catalyst Cu/HZSM5 presented gray color, attributed to the oxide copper (CuO) particles, located at the external surface of the support. The CuO particles are formed after calcination of the $(CuOH)^{+}$ and $(CuOH)^{2+}$ species generated by hydrolysis of the Cu^{2+} ions during the pH adjustment. Regarding the catalysts supported on alumina, the blue color was attributed to the presence of hydrated octahedral complexes of copper ions (Cu^{2+}).

Table 2 presents the results of the textural properties. The based like-hydrotalcite catalyst showed adsorption/desorption isotherms, which are typical of mesoporous materials. Comparing the textural properties of this catalyst Cu/Mg–Al with the support Mg–Al, it shows a big increase of the BET area, due to the increasing mesoporosity. This increase was attributed to the calcination process, due to the destruction of the like-hydrotalcite structure, accompanied by ion carbonate transformation in CO_2, resulting in the formation of new mixed oxides of magnesium, aluminum and copper oxides, displaying surface areas seven-fold bigger than the supports. On the other hand, the surface areas, micro- and mesoporous volumes of the Cu/HZSM-5 and Cu/γ-Al_2O_3 catalysts did not change with insertion of copper, showing that the structure of the support was preserved. The small decrease of these parameters can be attributed to partial and/or total blockage of the micro- and mesoporous by CuO particles.

3.2. Structure-X-ray diffractogram

XRD measurements were performed aiming to determine the phase composition of the catalysts, as displayed in figure 1. Results show that the addition of the metal causes a decrease in the peak intensity of the Cu/HZSM5 catalyst (figure 1a and b), as well as in the alumina supported catalyst (figure 1e and f), without crystalline loss, in agreement with the BET surface area results; therefore, there are no structural modifications of the supports. Moreover, the diffraction patterns show typical peaks of CuO particles, justifying the decreasing surface area of these samples. The Cu/Mg–Al diffractions (figure 1c and d) show the collapsing of the like-hydrotalcite structure, due to the disappearance of characteristic peaks of the like-hydrotalcite structure (11.5°; 22.9°; 34.5°; 45.7°; 60.4°; 61.7°) and the appearance of new peaks, a new material, corresponding to mixed oxides (MgO and CuO). These two phases were observed through peaks 43.4° and 62.9°, which are characteristic of the MgO-periclase, while the phase CuO-tenorite, with little crystalline structure, was observed on the Cu/Mg–Al sample (peaks at 37.5°; 39.5°). These results agree with the N_2 physisorption data.

3.3. Temperature-programmed reduction – TPR

The figure 2a–c displays the TPR results. According to the literature copper is reduced successively with an intermediary step ($Cu^{2+} \rightarrow Cu^{1+} \rightarrow Cu^{0}$ and $CuO \rightarrow Cu^{1+} \rightarrow Cu^{0}$). To Beutel *et al.* [10] there are three reduction peaks: at 298 K, which is associated to the reduction of the $[Cu–O–Cu]^{2+}$ species; at 498 K assigned to the reduction of species $Cu^{2+} \rightarrow Cu^{1+}$ and $CuO \rightarrow Cu^{0}$ and finally around 543 K associated to the reduction of species $Cu^{1+} \rightarrow Cu^{0}$. The absence of any peak at room temperature indicates that all samples do not present $[Cu–O–Cu]^{2+}$ species. The Cu/HZSM5 catalyst (figure 2a) exhibited two peaks at 548 and 686 K. Regarding to the preparation (ionic exchange followed by precipitation with ammonia) and considering that the hydrogen consumption was 40% greater in the first peak than in second one, it may be inferred that at 548 K occurs the reduction of $Cu^{2+} \rightarrow Cu^{1+}$ and $CuO \rightarrow Cu^{0}$ and at 686 K the reduction of $Cu^{1+} \rightarrow Cu^{0}$.

The reduction profile of Cu/Mg–Al catalyst discards the presence of copper under oxocations form due to absence of H_2 consumption at room temperature.

Table 2
Textural characterizations values of the samples

Catalysts	Area (m^2/g_{cat})		V_{micro} (cm^3/g_{cat})	V_{meso} (cm^3/g_{cat})	$\bar{d}_p$ (Å)	Isotherms
	BET	Microporos				
HZSM5	378.7	363.0	0.170	–	–	I
Cu/HZSM5	322.6	309.6	0.140	–	–	I
Mg–Al	29.9	28.1	–	0.157	158.9	IV
Cu/Mg–A1	225.8	0	–	0.494	85.7	IV
γ-Al_2O_3	185.1	6.6	–	0.456	97.4	IV
Cu/Al_2O_3	180.9	12.3	–	0.429	93.7	IV

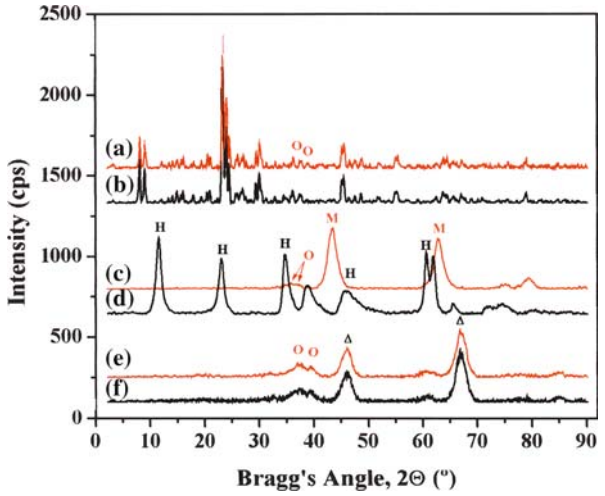

Figure 1. XRD patterns of the catalysts: (a) Cu/HZSM5, (b) HZSM5, (c) Cu/Mg–Al (d) Mg–Al (e) Cu/Al_2O_3 and (f) Al_2O_3 (O → CuO; Δ → γ-Al_2O_3; M → MgO; H → Like-hydrotalcite).

Regarding the reduction peaks the first one was attributed to the reduction of $CuO \rightarrow Cu^0$ and the second and third peak were attributed to the reduction of copper species with different reducibility, which were not detected in the XRD spectra, probably due to the great dispersion or small crystallite sizes of the oxide mixture. DRS data confirm these conclusions, where oxications species were not observed, however, small clusters highly dispersed of oxide mixtures and small amounts of the Cu^{+2} species in tetrahedral coordination were identified [13].

The Cu/alumina supported catalyst presented a different behavior. It displays two reduction peaks (figure 2c), which are attributed to the successive reduction of copper. The first peak is due to the reduction of $CuO \rightarrow Cu^{1+}$ together with the reduction of $CuO \rightarrow Cu^0$, because the hydrogen consumption of the first peak was 52% greater than the second one, while the second peak was related to the reduction of $Cu^{1+} \rightarrow Cu^0$.

3.4. Temperature-programmed desorption – TPD-NH_3

The TPD-NH_3 technique was used to investigate the site density and strength acid sites of the catalysts. According to the literature, desorption temperatures below 673 K are weak acid sites, while above this temperature they are classified as strong acid sites [17]. Thus, analyzing the profiles (figure 3a–c) and the amounts of ammonia desorption, the Cu/HZSM5 catalyst presents high acid density and two different acid sites. The first one at 555 K is attributed to weak acid sites (Lewis sites), of the order of 93% ($4,528 \times 10^{-1}$ $gmol_{NH_3}/g_{cat}$) of the total acidity and the second one at 777 K corresponds to strong acid sites (Brönsted sites), 7% ($3,387 \times 10^{-2}$ $gmol_{NH_3}/g_{cat}$) of the total acidity. The Cu/Mg–Al and Cu/Al_2O_3 samples displayed only one peak of desorption at 537 K ($1,374 \times 10^{-3}$ $gmol_{NH_3}/g_{cat}$) and 477 K ($1,132 \times 10^{-2}$ $gmol_{NH_3}/g_{cat}$), respectively, which can be attributed to weak and moderate acid sites (Lewis sites). The acidity of the Cu/Mg–A1 catalyst is low due to the basic character of support.

3.5. Reactivity

The reaction was performed by temperature-programmed surface reaction in two different ways: first, pre-adsorption of ammonia and then methanol flux; secondly, pre-adsorption of methanol and then ammonia flux. In the preferential adsorption of NH_3 or CH_3OH there are big differences with the supports (figure 4a–f).

In the first case with pre-adsorption of NH_3 and methanol flux the results (figure 4a, c and e) show at low temperature only formation of MMA, and increasing

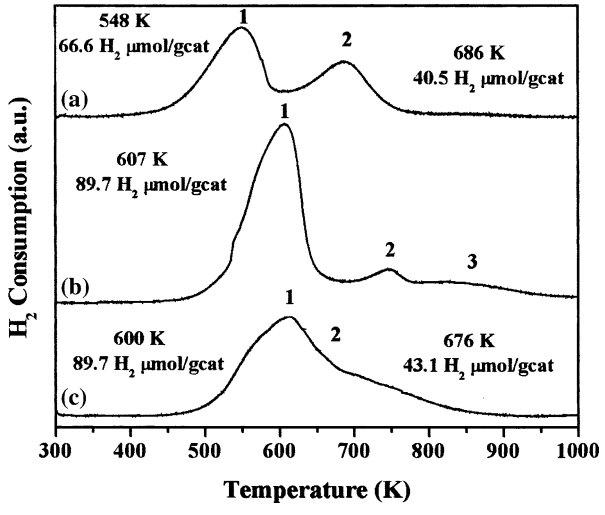

Figure 2. TPR profile for different catalysts: (a) Cu/HZSM5 (b) Cu/Mg–Al and (c) Cu/Al_2O_3.

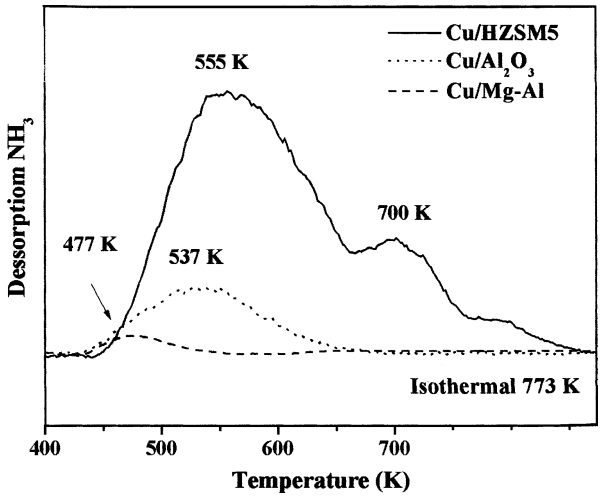

Figure 3. TPD-NH_3 profiles of the different cataysts.

the temperature it favors the production of the other methylamines (DMA and TMA), which appeared at 500 K, with simultaneous consumption of MMA, due to reaction sequence, as described in equations (1)–(3). The methylamine profile is not a well-defined peak and must be seen with caution. In the second case, with methanol pre-adsorption and NH_3 flux (figure 4b, d and f), desorption products occurred in well-defined peaks (mainly for MMA) at low temperatures on HZSM5 and Mg–Al supports. However, the γ-Al_2O_3 supported catalysts showed two zones for methylamine formation (MMA and DMA): 370–400 K and 660–680 K, suggesting that there are active sites with different strengths.

These results showed that during the pre-adsorption ammonia is strongly attached at the surface sites with prevailing formation of a sublayer, which hinders the subsequent methanol adsorption and hence the reaction

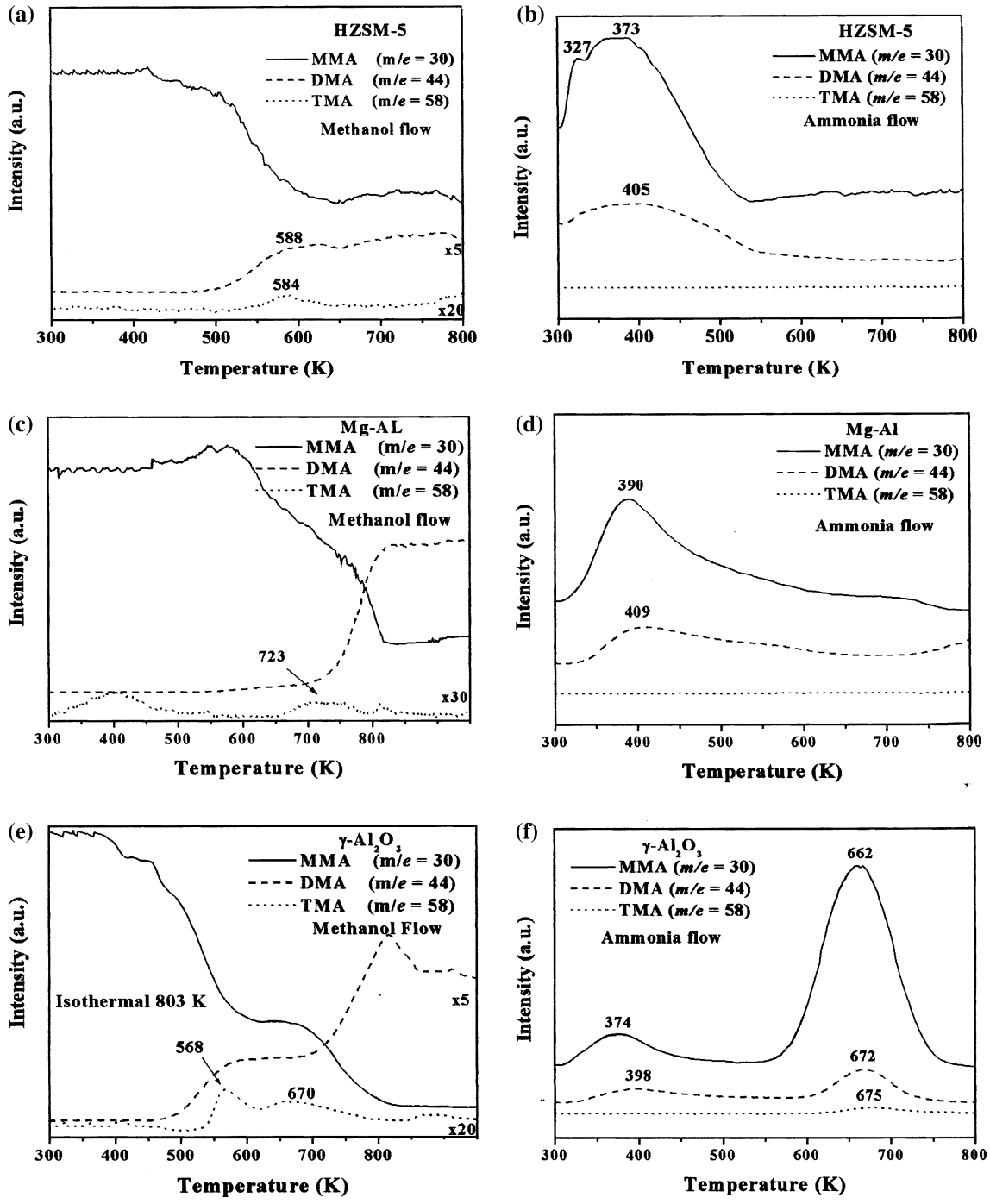

Figure 4. TPSR profiles of the supports, performed by two different experimental procedures: (a, c and e – methanol flow) and (b, d and f – ammonia flow).

to methylamines (DMA and TMA). In this case, the reaction may occur between adsorbed ammonia molecules and adsorbed methanol molecules (responsible for the formation of DMA and TMA) or between adsorbed ammonia and methanol in gas phase (formation of MMA).

These results showed the dependence of the surface acid and base properties, which can be explained analyzing of the basicity of the reactants (ammonia and methanol). The higher basicity of ammonia can easily displace the weakly adsorbed methanol molecules, and therefore the amination reaction of methanol occurs through ammonia adsorbed on weak, moderate or strong sites (in case of pre-adsorption) with methanol molecules strongly adsorbed or in gas phase. With methanol pre-adsorbed it seems that only a small amount remain adsorbed and the molecules are released in the gas phase. That suggests that the reaction is difficult, because the contact time between reactants is too short, as seen in figure 4a, c and e, where peaks are not well defined. With ammonia pre-adsorbed the contact time is favored due to the formation of an ammonia sublayer at the surface and because methanol is in excess in gas phase, as shown in figure 4b, d and f on well-defined peaks.

$$CH_3OH + NH_3 \Leftrightarrow MMA + H_2O \quad (1)$$

$$MMA + NH_3 \Leftrightarrow DMA + H_2O \quad (2)$$

$$DMA + NH_3 \Leftrightarrow TMA + H_2O \quad (3)$$

Comparing the TPSR profiles of the supports with the corresponding copper catalysts, as shown in figure 5a, c and e (methanol flow) and figure 5b, d and f (ammonia flow), it turns out that they are very similar concerning the desorption of the main products on both cases. The two peaks of based like-hydrotalcite catalysts are identical for the main product (DMA), varying only in intensity in the different experimental procedures. The same behavior was observed for the alumina supported catalysts. Therefore, one can conclude that for the Cu/Mg–Al catalysts the sequence of reactant adsorption does not interfere in the methylamine formation. On the other hand, when ammonia is pre-adsorbed on the alumina-supported catalysts, the desorption temperature increases with increasing temperature.

It suggests that the strong pre-adsorbed reactant forms a sublayer or monolayer reacting with the gas phase reactant, according to the Rideal–Eley surface reaction mechanism. Indeed, comparing the TPD results of ammonia and methanol, it turns out that the affinity of ammonia is lower than of methanol (not shown) for the based like-hydrotalcite catalyst, and the desorption of the products is facilitated, as shown comparing figure 5c and d. However, for the alumina-supported catalysts, the affinity of ammonia is greater than of methanol.

On the other hand, the Cu/HZSM5 catalyst showed significant differences of the desorption profiles, being DMA the main product, when the experiment was performed using methanol flux, however, with an ammonia flux the MMA was the main product, showing that the sequence of pre-adsorption of the reactants interfere in the methylamine distribution, in agreement with the results reported by Nunes *et al.* [8].

The suggested distribution of methylamines are observed by FTIR spectroscopy with reaction *in situ* (figure 6). According to line A, methanol is not adsorbed, while line B exhibits band 1625 cm^{-1}, which corresponds to the adsorption of ammonia, which is attributed to the adsorption on Lewis acid sites. It suggests prevailing adsorption of ammonia. Starting the reaction (line C) it exhibits one band at 1602 cm^{-1} which is assigned to monomethylamine, linked to the Lewis acid sites [14].

The disproportionation reactions of MMA to DMA and TMA were also observed, according to equations (4–6), as shown in (figure 5a, c and f), displaying the consumption of MMA and the formation of the DMA and TMA, with a maximum with increasing temperature, as reported by Balker *et al.* [15].

$$2MMA \Leftrightarrow DMA + NH_3 \quad (4)$$

$$MMA + DMA \Leftrightarrow TMA + NH_3 \quad (5)$$

$$2DMA \Leftrightarrow TMA + MMA \quad (6)$$

The methanol amination reaction was tested, measuring the methanol conversion and partial selectivity between methylamines (MMA, DMA and TMA). The effect of temperature (573–773 K) is presented in table 3. The methanol conversion increases with temperature increase, mainly for the Cu/Al_2O_3 and Cu/HZSM5 catalysts. These results can be explained due to the basic character of the products and the strong acidity of the catalysts, as shown in the TPD-NH_3 and FTIR-Py results. It suggests that at low temperature, the products remain partially adsorbed and with increasing temperature the desorption is easy, favoring the methanol conversion, in accordance with the results reported by Ilao *et al.* [5]. The activity was compared at isoconversion (25%), indicating the following order: $Cu/Al_2O_3 > Cu/HZSM5 > Cu/Mg–Al$. Mochida *et al.* [16] studied the methylamine synthesis on different zeolites with transition metals, and concluded that the acid sites strength affected the activity. Then, despite the Cu/HZSM5 catalyst contains much stronger acid sites than the Cu/Al_2O_3 catalyst, the later one exhibits better activity, indicating that the reaction proceeds through moderate acid strength.

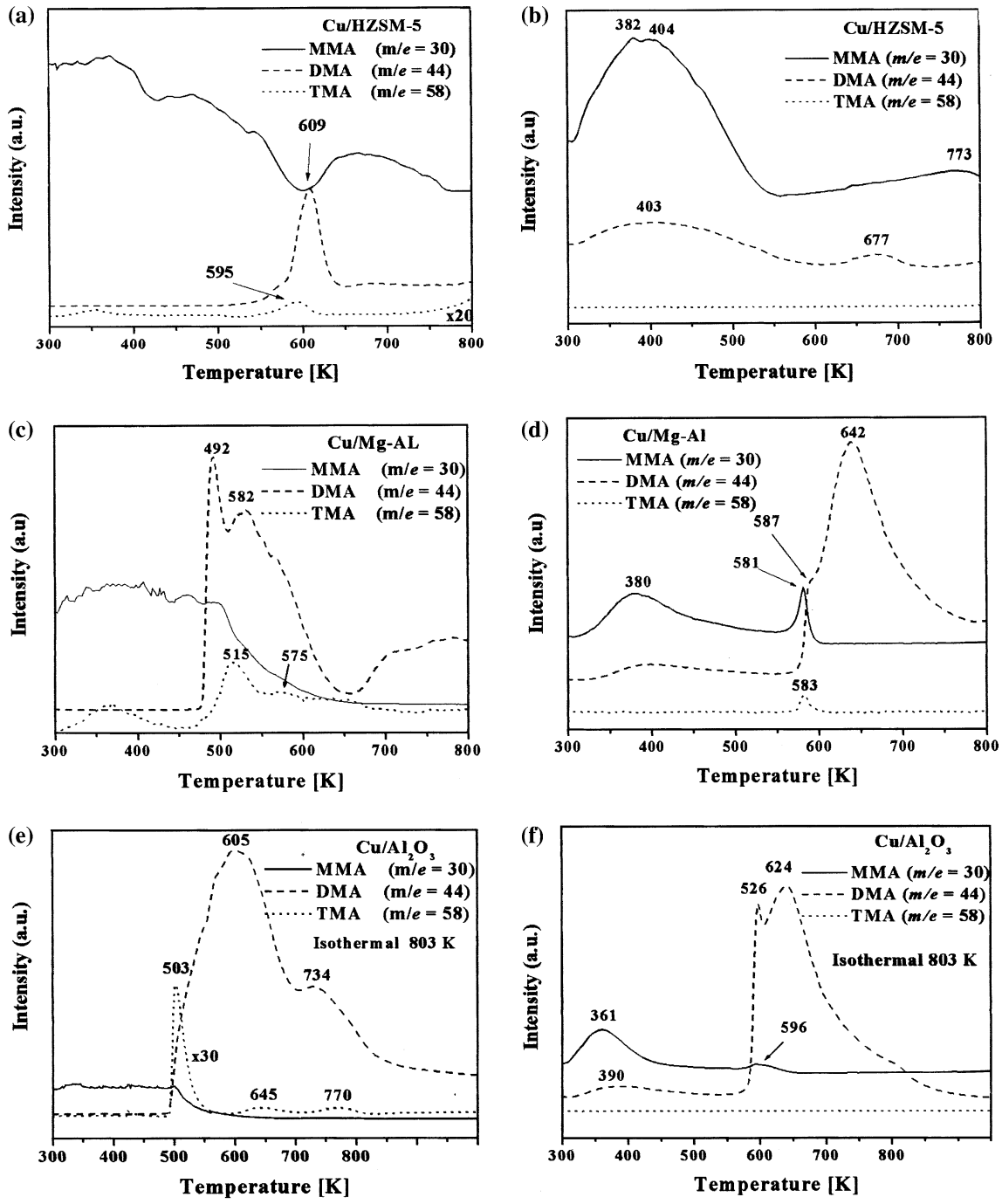

Figure 5. TPSR profiles of different catalysts the two methodology: methanol flux (a) Cu/HZSM5, (c) Cu/Mg–Al and (e) Cu/Al_2O_3. Ammonia flux (b) Cu/HZSM5 (d) Cu/Mg–Al and (f) Cu/Al_2O_3.

The selectivity was obtained at isoconversion and is displayed in table 3. The Cu/HZSM5 catalyst was the most selective for methylamine, with the formation of fewer by-products, in comparison with the Cu/Mg–Al. The Cu/HZSM5 catalyst presented also more DMA at different temperatures, displaying maximum selectivity with increasing temperature, due to the sequential reaction as described in equations (1)–(3), in accordance with reported results of Ilao *et al.* [5]. With copper like-hydrotalcites the selectivity of MMA was 100%, however, the production was lower compared to the other catalysts, because of the formation of different other by-products (not methylamines). The explanation for the preferential formation of MMA is related to the weak acid sites (basic solid) and the faster desorption, avoiding the sequential formation of DMA and TMA. Comparing the selectivity to MMA at isoconversion of the different catalysts, we obtain the same above sequence as for the activity. Carja *et al.* [7] studied the methylamine synthesis with copper like-hydrotalcites

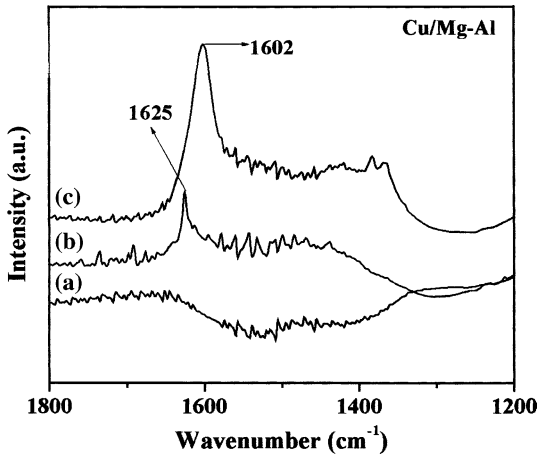

Figure 6. Infrared FTIR spectroscopy with *in situ* of reaction for the 7Cu/Mg–Al catalyst. (a) adsorption of methanol; (b) Adsorption of ammonia and (c) reaction *in situ* at 623 K.

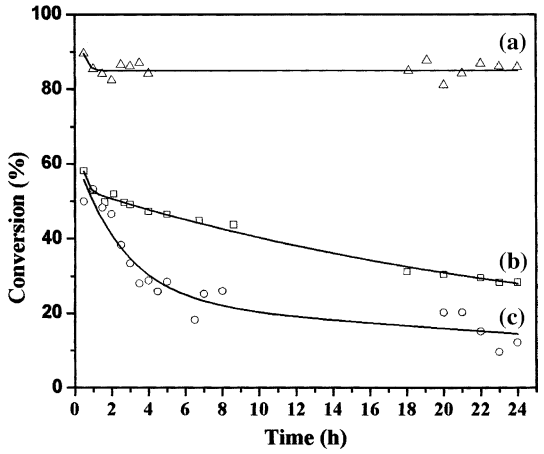

Figure 7. Stability test for (a) Cu/Al_2O_3, (b) Cu/Mg–Al and (c) Cu/HZSM5.

and observed that with increasing temperature MMA formation is also favored.

The stability test was carried out at 773 K, 1 atm and molar ratio (N/C = 1) in feed composition during 24 h. The deactivation of the Cu/HZSM5 catalyst (figure 7c) is significant, compared to the other catalysts, decreasing sharply after 6 h with time on stream (methanol conversion decreased from 53% to 13%), in contrast to previous results of Nunes *et al.* [8] for the 3.7% Cu/HZSM5 catalyst, after 8 h with time on stream. The Cu/Mg–Al catalyst (figure 7b) deactivated approximately 30% due to coke deposition. Depending on the support the reaction favors the formation of higher hydrocarbons (C3–C6), which are the precursors of coke. Cu/Al_2O_3 catalyst (figure 7a) was very stable, which can be attributed to the moderate acid sites, as shown in the TPD-NH_3 and FTIR-Py results and the textural properties, favoring the desorption of products and avoiding any diffusion impediment, respectively.

According to the literature, the deactivation on Cu-based catalysts on the methanol amination reaction occurs either by coke formation and/or formation of a monolayer of nitrides due to the methylamine disproportionation reaction. From the experimental results the last one can be disregarded, because copper nitrides decompose above 600 K on nitrogen atmosphere [17].

4. Conclusions

The loss of surface area of Cu/alumina and Cu/zeolite can be attributed to the formation of CuO particles, blocking pores. Contrary, the based like-hydrotalcite catalysts surface areas increased, due to the destruction of the structure and the formation of oxide mixtures. TPD-NH_3 showed that the Cu/HT presents weak acid sites, contrasting with the Cu/ZSM5 catalyst.

TPSR results showed that the insertion of copper decreased the temperature of desorption of methylamines, but favored the disproportionation reactions.

Table 3
Catalytic data of the differents catalysts

Catalysts	Temp. (K)	X_{CH3OH} (%)	SP_{MMA} (%)	SP_{DMA} (%)	SP_{TMA} (%)	MMA (μmol)	DMA (μmol)	TMA (μmol)
Cu/HZSM5	573	5.68	66.3	0	33.7	3.5	0	1.8
	623	17.7	38.7	21.0	40.2	4.7	2.5	4.9
	673	43.1	26.9	24.1	48.9	7.4	6.6	13.5
	723	71.6	29.4	31.7	38.9	10.8	11.7	14.3
	773	66.6	34.6	32.0	33.3	15.5	14.4	15.3
Cu/Mg–A1	573	8.52	100	0	0	3.1	0	0
	623	15.1	100	0	0	3.3	0	0
	673	18.5	100	0	0	3.8	0	0
	723	23.4	100	0	0	5.0	0	0
	773	40.1	100	0	0	6.2	0	0
Cu/Al_2O_3	573	20.1	100	0	0	15.0	0	0
	623	73.8	97.6	0	2.37	50.0	0	1.2
	673	79.9	84.8	6.54	8.57	35.9	2.7	3.6
	723	91.3	42.2	20.8	36.91	11.4	5.6	10.0
	773	98.3	26.5	22.8	50.5	4.8	4.1	9.2

There are preferential adsorptions of the reactants on the acid sites of the alumina and HZSM5 catalysts. On the contrary, the metallic sites of the based liked-hydrotalcite catalysts favored methylamines formation.

The Cu/Al_2O_3 sample was very active and stable, with 98% methanol conversion without significant deactivation. On the contrary the Cu/HZSM and Cu/HT catalysts showed fast deactivation due to coke deposition.

The Cu/HT presented very high selectivity (100%) to MMA, besides more by products other than methylamines, which results in a smaller production when compared the other catalysts.

References

[1] S.V. Gredig, R.A. Koeppel and A. Baiker, Appl. Catal. A 162 (1997) 49.
[2] D.R. Corbin, S. Schwarz and G.C. Sonnichsen, Catal. Today 37 (1997) 71.
[3] M. Pérez-Mendoza, M. Domingo-Garcia and F.J. Lóez-Garzón, Appl. Catal. A 224 (2002) 239.
[4] K.S. Hayes, Appl. Catal. A 221 (2001) 187.
[5] M.C. Ilao, H. Yamamoto and K. Segawa, J. Catal. 161 (1996) 20.
[6] S.M. Auer, S.V. Gredig, R.A. Koeppel and A. Baiker, J. Mol. Catal. A 141 (1999) 193.
[7] G. Carja, R. Nakamura and H. Niiyama, Appl. Catal. A 236 (2002) 91.
[8] M.H.O. Nunes, V.T. Silva and M. Schmal, Catal. Lett. 97 (2004) 1.
[9] A.C.C. Rodrigues, C.A. Henriques and J.L.F. Monteiro, Actas XVIII Simpósio Iberoamericano de Catálisis 1 (2002) 2009.
[10] T. Beutel, J. Sarkany, G.D. Lei, J.Y. Yan and W.M.H. Sachtler, J. Phys. Chem. 100 (1996) 845.
[11] F. Kovanda, K. Jirátová, J. Rymeš and D. Koloušek, Appl. Clay Sci. 18 (2001) 71.
[12] S.M. Auer, R. Wanderler, U. Göbel and A. Baiker, J. Catal. 169 (1997) 1.
[13] B. Montanari, A. Vaccari, M. Gazzano, P. Käßner, H. Papp, J. Pasel, R. Dziembaj, W. Makowski and T. Lojewski, Appl. Catal. B 13 (1997) 205.
[14] E. Jobson and A. Baiker, J. Chem. Soc. Faraday Trans. 86 (1990) 1131.
[15] A. Baiker, W. Caprez and W.L. Holsteins, Ind. Eng. Chem. Prod. Res. Dev. 22 (1983) 217.
[16] I. Mochida, A. Yasutake, H. Fujitsu and K. Takeshita, J. Catal. 82 (1983) 313.
[17] A. Balker and M. Maciejewski, J. Chem. Soc. Faraday Trans. 80 (1983) 2331.